

WiPd: Contactless Water-Injected Pork Detection Using Commodity WiFi Devices

^{ab}Pengming Hu, ^{a†}Weidong Yang, [§]Xuyu Wang, [‡]Shiwen Mao and [†]Chao Niu

^aHenan Key Laboratory of Grain Photoelectric Detection and Control, Henan University of Technology, Zhengzhou, 450001, China

^bCollege of Mechanical and Electrical Engineering, Henan University of Technology, Zhengzhou, 450001, China

[†]College of Information Science and Engineering, Henan University of Technology, Zhengzhou, 450001, China

[§]Knight Foundation School of Computing and Information Sciences, Florida International University, Miami, FL 33199, USA

[‡]Department of Electrical and Computer Engineering, Auburn University, Auburn, AL 36849-5201, USA

hupengming@stu.haut.edu.cn, Yangweidong@haut.edu.cn, wangxuyu316@gmail.com, smao@ieee.org, niuchao@stu.haut.edu.cn

Abstract—Detection of water-injected pork is of great significance for pork safety and food quality monitoring. In this paper, we propose a nondestructive wireless sensing system, termed WiPd, for rapid detection of water-injected pork using commercial WiFi devices. We first verify the feasibility of water-injected pork detection using WiFi channel state information (CSI). We then design the WiPd system consisting of a sensing module, a preprocessing module, and a detection model module. In the sensing module, commercial WiFi devices are used to collect different types of CSI data from normal pork and water-injected pork. In the data preprocessing module, the CSI ratio model is used to eliminate the environment and hardware noise, and then the subcarrier selection and normalization methods are carried out for feature extraction. In the detection module, a double-layer long short-term memory (LSTM) network is designed to detect water-injected pork with an online detection method. Finally, we evaluate the proposed WiPd system with extensive experiments, and the results show that WiPd can achieve an average detection accuracy of more than 98% in line-of-sight (LOS) scenarios.

Index Terms—Channel State Information (CSI), Water-injected pork detection, CSI ratio, Long short-term memory (LSTM).

I. INTRODUCTION

Pork has always represented an important part in meat and meat products in many countries, as one of the most favorite meat in people's daily diets. However, its adulteration has raised a lot of concerns [1], [2]. Adulteration generally happens in two ways. The first is to use inferior pork as high-quality pork, while the other is to increase the weight of pork by means of water injection. Water injection has been widely exploited for benefits, because there is no technical hurdle for injecting water into pork, as well as no cost incurred for adulteration. However, when pork is injected with water, its freshness will be degraded, and it will become more prone to deterioration, causing the loss of nutrients and finally reducing or even losing its use value. In order to protect the interest of consumers and maintain the fairness of the market, detection of water-injected pork is of great practical importance.

The traditional moisture detection methods mainly include the drying method [3] and the distillation method [4]. Because

of the time-consuming and complex operations, they are not suitable for wide use in the meat market. In addition, the methods of rapid moisture detection can also be applied to meat, such as the nuclear magnetic resonance method [5], the near infrared reflection method [6], the spectral imaging method [7], and the microwave method [8], etc. These existing methods can be used for nondestructive and rapid detection of meat moisture. However, the expensive equipment makes it hard to deploy them in the meat market. Therefore, a low-cost, fast and effective detection method is in urgent demand.

Recently, the WiFi based wireless sensing technology has received extensive attention. For example, WiFi received signal strength (RSS) has been used for some simple sensing tasks (e.g., indoor positioning) as a kind of coarse channel information [9]. Moreover, channel state information (CSI) of the WiFi physical layer can also be extracted from some commercial WiFi network interface cards (NIC), including CSI amplitude and phase information. WiFi CSI represents fine-grained channel information than RSS, which can better capture the characteristics of channel (e.g., attenuation, distortion, and reflections). Consequently, WiFi CSI have been used in many radio frequency (RF) sensing systems for smart health [10], indoor positioning [11], environmental monitoring [12], human-computer interaction (HCI) [13], and smart farming [14]–[16].

Motivated by above RF sensing systems, in this paper, we propose a water-injected pork detection system based on WiFi CSI, which provides a low-cost, fast and effective detection method. When pork is injected with water, the change of its moisture will cause measurable changes in WiFi CSI measurements. In this paper, we first verify the feasibility of using CSI data for detection of water-injected pork. The experimental results show that both the amplitude and phase of CSI before and after water injection are sufficiently different, and thus can be used for classification of normal and water-injected pork.

In particular, we design a water-injected pork detection system using WiFi CSI, termed WiPd. The WiPd system does not require expensive special equipment and is easy for

deployment. The WiPd system design includes three modules. The first is the sensing module, which focuses on CSI data collection. The second is the data preprocessing module. We use the CSI ratio model, which not only greatly mitigates the environment and hardware noise, but also retains the channel characteristics. In addition, we choose the CSI subcarriers that have lower noises, and then normalize the CSI ratio data. The detection model is established in the third module. Although the CSI ratio samples before and after water injection are different, some samples could still be similar. In this paper, we exploit a double-layer long short-term memory (LSTM) network to achieve high detection accuracy with preprocessed CSI ratio data. Finally, the trained model will be used for water-injected pork detection with an online detection method.

The main contributions of this paper are summarized below:

- We verify the feasibility of using WiFi CSI for water-injected pork detection. To the best of our knowledge, this is the first work to use WiFi CSI sensing for water-injection pork detection.
- We design the WiPd system, including the sensing module for CSI data collection, the data preprocessing module using CSI ratio model, and the detection model module with a double-layer LSTM.
- We use commercial WiFi devices to prototype the WiPd system. The experimental results show that the proposed WiPd system can detect water-injected pork with an average accuracy of over 98% in the line-of-sight (LOS) scenario. We also validate the effectiveness of WiPd under different system parameters and environments.

The remainder of this paper is organized as follows. The preliminaries and feasibility are presented in Section II. We describe the WiPd system design in Section III and evaluate its performance in Section IV. Section V concludes this paper.

II. PRELIMINARIES AND AND FEASIBILITY

A. Water-injected Pork Detection

The rapid detection of water-injected pork is a challenging problem. Generally in the food market, the completion time of pork trading between merchants and consumers is quite short. Thus, it is necessary to develop water-inject pork detection techniques to quickly detect the adulteration.

Generally, the moisture content of normal pork is about 77%. Based on the threshold, moisture content detection methods can be used to identify water-injected pork. For example, the drying method is a traditional moisture content detection technique, which assess the moisture content by measuring the change of weight before and after drying [3]. The direct drying method has a higher accuracy in moisture content detection, but it is destructive to the pork itself, as well as being time-consuming and labor-consuming. Thus, this method cannot meet the requirements of on-site, fast detection. Distillation methods [4] steam the water, toluene, and xylene in the sample through a water tester utilizing the physical and chemical properties of water, and then calculate the water content in the test sample as the volume of water. However, this method also

destroys the pork itself. In addition, the test results may also produce detection errors due to incomplete volatilization of water in the sample, as well as the attachment of water on the surface of the instrument. Therefore, the distillation methods cannot be applied to the rapid detection of water-injected pork.

In addition to traditional methods, several more recent techniques are developed to address the above issues as well (e.g., destruction of samples and long detection time). For example, near infrared reflectance spectroscopy has been used to determine the moisture content of fresh meat [6], while hyperspectral imaging analysis has been exploited to identify water-injected meat samples [7]. In [5], nuclear magnetic resonance data and multivariate analysis were utilized to detect the moisture content of meat. These methods are nondestructive and can rapidly detect meat moisture. However, the testing equipment of these methods is expensive (e.g., a hyperspectral instrument usually costs tens of thousands of dollars), making them only suitable for testing in a laboratory rather than widely deployed in the food market. Therefore, in order to protect the interests of consumers, a low-cost, fast and effective detection method will be highly desirable.

B. Channel State Information

Recently, more and more commercial WiFi network cards, such as the Intel 5300 NIC, the Atheros 9380 NIC, and the ax210 NIC provides the CSI of the physical layer. For example, CSI data from 30 subcarriers can be read from each antenna fro each received packet with the Intel 5300 NIC. In this paper, we use the PicoScenes platform to obtain CSI from 57 subcarriers by interpolating the original CSI data from 30 subcarriers to improve the performance of WiFi sensing [17]. More CSI subcarriers are helpful to achieve a higher accuracy, especially for complex tasks. The cost of the commercial Intel 5300 NIC used in this paper is much lower (i.e., only about \$25) than those used in the existing methods.

Using the commodity WiFi NIC with modified firmware and device driver, CSI data, such as amplitude and phase, can be extracted from each of the N_s CSI subcarriers. Specifically, the collected dataset contains the number of transmitting antennas N_{tx} , the number of receiving antennas N_{rx} , the packet transmission frequency f , and CSI data \mathbf{H} . CSI data \mathbf{H} can be represented as an $N_{tx} \times N_{rx} \times N_s$ tensor, denoted by

$$\mathbf{H} = (H_{ijk})_{N_{tx} \times N_{rx} \times N_s}. \quad (1)$$

In our WiPd system, CSI data from 57 subcarriers are collected at a 5GHz with for a 20MHz WiFi channel at the 5GHz band using the Intel 5300 NIC. The k th subcarrier data in \mathbf{H} corresponding to a transmitting and receiving antenna pair can be defined by

$$H_k = A_k e^{j\angle\phi_k}, \quad (2)$$

where A_k and $\angle\phi_k$ are the amplitude and phase of the CSI data from the k th subcarrier, respectively.

C. Feasibility of the Proposed Approach

To verify the feasibility of using CSI data for water-injected pork detection, we collect CSI data from four different pork samples and extract the amplitude and phase data. The moisture contents of two kinds of pork samples without water-injection are 77% and 76.68%, respectively, and the moisture contents of two kinds of water-injected pork samples are 80.22% and 81.28%, respectively. In the experiments, the critical moisture content of pork is set to 77%, because the moisture content of normal pork is $\leq 77\%$, and that of water-injected pork is usually $>77\%$.

The CSI amplitude and phase data from pork samples with 76.68%, 76%, 80.22%, and 81.28% moisture content are collected and presented in Figs. 1 to 6. The original CSI amplitude data are shown in Fig. 1 to Fig. 3. Fig. 1, shows that the CSI amplitude of the pork sample close to normal is very similar to that of the normal pork sample. In Fig. 2 and Fig. 3, we can see that the CSI amplitude becomes very different after the pork is injected with water. In addition, Fig. 4 to Fig. 6 show the unwrapped CSI phase data collected from the four pork samples. Fig. 4 shows that the CSI phase data of close to normal pork sample is also similar to that of the normal port sample. After the pork is injected with water, there are small changes in CSI phase data, as shown in Fig. 5 and Fig. 6. These results demonstrate the feasibility of using CSI data to detect water-injected pork.

III. THE WIPD SYSTEM DESIGN

This section will introduce the WiPd system design. As shown in Fig. 7, the system architecture includes sensing, preprocessing, and the detection model. First, in the sensing phase, we use the Intel 5300 NIC to extract the amplitude and phase data from different pork samples. In the data preprocessing stage, we exploit the CSI ratio model to eliminate environment noise, and propose the subcarrier selection and data normalization methods for data preprocessing. Last, the detection model is established, where we build a double-layer LSTM network and conduct off-line training, and then use the new CSI data for water-injected pork detection using the trained model.

A. CSI Data Sensing

In the CSI data sensing stage, we use the Intel 5300 NIC to collect CSI data from 57 subcarriers with the PicoScenes platform. For different pork samples, we set the same experimental condition for data collection. Under other conditions, only different pork samples are used. We collect CSI data for four pork samples, and then extract the amplitude and phase for the detection of water-injected pork.

B. CSI Data Preprocessing

In the data preprocessing stage, we first use the CSI ratio model to eliminate environment noise and phase errors. Then we select the most stable subcarrier and normalize the data.

1) *CSI Ratio Model*: Recently, the CSI ratio model has been shown effective for canceling CSI amplitude and phase noises [18]. For example, the clock and carrier frequency offsets between the WiFi transmitter and receiver will lead to random phase offsets in different packets and introduce amplitude noise. The basic ideas of the CSI ratio model is to use two antennas of the WiFi receiver to remove the CSI phase and amplitude noise because usually both antennas experience the same levels of amplitude noises and phase offsets. Specifically, the amplitude noise and phase offset can be eliminated by using the ratio of the CSI data from two antennas (i.e., the CSI ratio), given by

$$H_r(f, t) = \frac{H_1(f, t)}{H_2(f, t)}, \quad (3)$$

where $H_1(f, t)$ is the CSI data collected from the first antenna, $H_2(f, t)$ is the CSI data collected from the second antenna. The advantage of using CSI ratio is that it can effectively eliminate the amplitude noise and phase offset introduced by the WiFi hardware.

Next, we apply the model to obtain the channel ratio between the two antennas, which is given by

$$\begin{aligned} \frac{H_1(f, t)}{H_2(f, t)} &= \frac{A(f, t)e^{-j2\pi\Delta\theta(f, t)}H_{\text{pork1}}(f, t)}{A(f, t)e^{-j2\pi\Delta\theta(f, t)}H_{\text{pork2}}(f, t)} \\ &= \frac{H_{\text{pork1}}(f, t)}{H_{\text{pork2}}(f, t)}, \end{aligned} \quad (4)$$

where $A(f, t)$ is the scaling noise of CSI amplitude, $\Delta\theta(f, t)$ is the random offset of phase in CSI, and H_{pork1} and H_{pork2} represent the ideal sensing channel for pork samples from the transmitting antenna to the first and the second antenna of the receiver, respectively. Therefore, the CSI data ratio between the two antennas is

$$\frac{H_{\text{pork1}}(f, t)}{H_{\text{pork2}}(f, t)} = \frac{A_{k1}e^{j\angle\phi_{k1}}}{A_{k2}e^{j\angle\phi_{k2}}} = \frac{A_{k1}}{A_{k2}}e^{j(\angle\phi_{k1}-\angle\phi_{k2})}, \quad (5)$$

where A_{k1} and A_{k2} are the original amplitudes of the k th subcarrier on the first antenna and the second antenna, respectively, ϕ_{k1} and ϕ_{k2} are the original phase data of the k th subcarrier on the first and the second receiving antenna, respectively. It can be seen from (5) that the core of the CSI ratio model is to convert the ratio of CSI data collected by two adjacent antennas into the amplitude ratio and phase difference between a pair of adjacent antennas.

Fig. 8 and Fig. 9 present the amplitude and phase of the CSI ratio model sampled from the four pork samples with different moisture contents, respectively. In Fig. 8, it can be seen that most of the noise in the amplitude data sequence has been effectively eliminated after using the CSI ratio model, as indicated by the much smaller range of amplitude compared to that of the original CSI amplitude data in Fig. 1 to Fig. 3. This is also true for the phase data shown in Fig. 9. In addition, the CSI ratio retains the characteristics of WiFi CSI dynamics. For example, Fig. 8 and Fig. 9 show that, compared with the normal pork CSI ratio, the CSI ratio of amplitude and phase of water-injected pork are obviously different, which will be leveraged for water-injected pork detection.

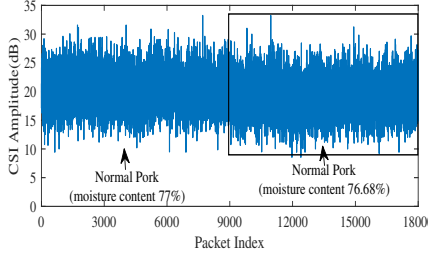


Fig. 1. CSI amplitude data for pork moisture contents of 77% and 76.68%.

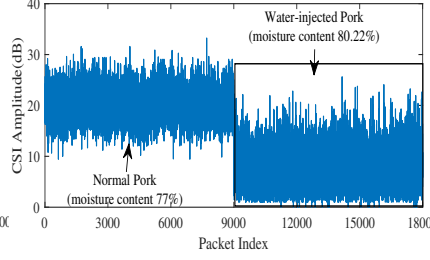


Fig. 2. CSI amplitude data for pork moisture contents of 77% and 80.22%.

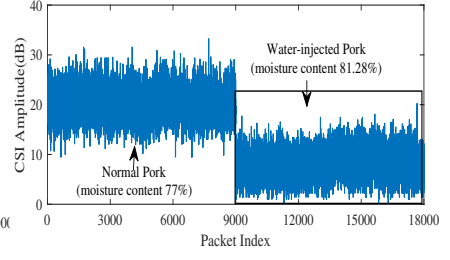


Fig. 3. CSI amplitude data for pork moisture contents of 77% and 81.28%.

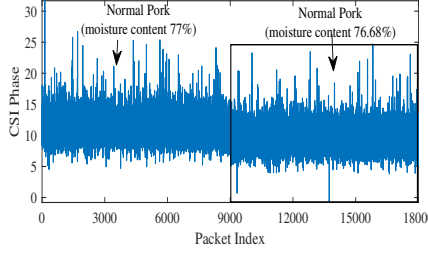


Fig. 4. CSI phase for pork moisture contents of 77% and 76.68%.

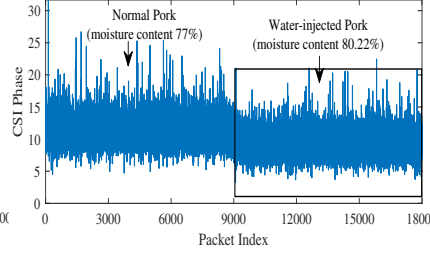


Fig. 5. CSI phase for pork moisture contents of 77% and 80.22%.

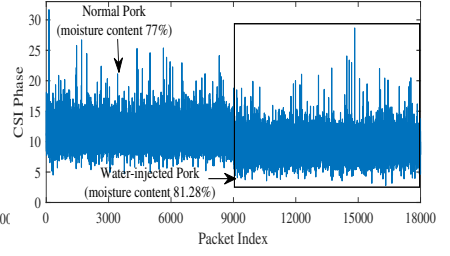


Fig. 6. CSI phase for pork moisture contents with 77% and 81.28%.

2) *Subcarrier Selection*: Although we employ the CSI ratio model to remove most of the noise, there could still be a small number of anomaly samples in CSI ratio data in practice. This is because in a typical indoor environment, the collected CSI data will be generally affected by multipath propagation, thus influencing the CSI ratio data.

To address this problem, we select the CSI subcarrier data with a smaller variance (e.g., less affected by multipath [19]). Specifically, for M receiving packets, the variance of the k th subcarrier, denoted by ϖ_k^2 , is given by

$$\varpi_k^2 = \frac{1}{M} \sum_{m=1}^M (H_k(m) - \bar{H}_k)^2, \quad (6)$$

where H_k represents the CSI ratio amplitude or phase data in the k th subcarrier, and \bar{H}_k is the mean of the CSI ratio amplitude or phase data in the k th subcarrier. Then, we rank the subcarriers according to ϖ_k^2 in the ascending order, and select the half of the subcarrier data with smaller variances as the input data of the detection model.

3) *Normalization*: To speed up the computation of the model and improve the detection accuracy of the WiPd system, we apply the zero-mean normalization method to the CSI ratio data. The normalized data V_k is calculated by

$$V_k = \frac{(H_k - \bar{H}_k)}{\varpi_k}. \quad (7)$$

The normalized data will be used as input features to the following deep learning model.

C. Detection Model

After data preprocessing, a double-layer LSTM network model is used to detect water-injected pork. It includes two

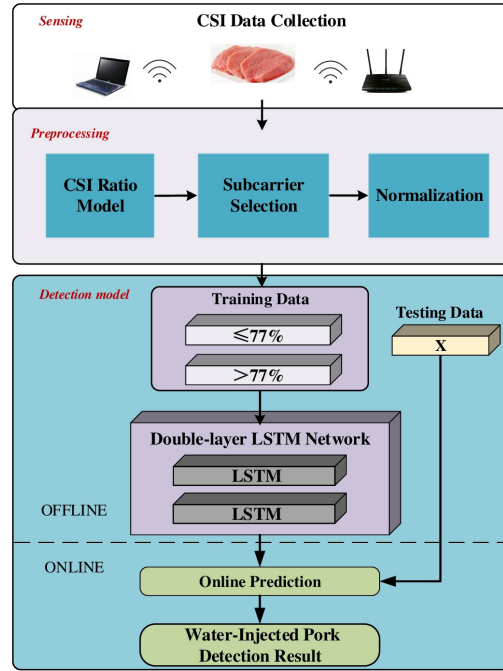


Fig. 7. Architecture of the proposed WiPd system.

stages: off-line training and on-line detection. The detection model consists of a double-layer LSTM network and a Soft-max classifier as follows.

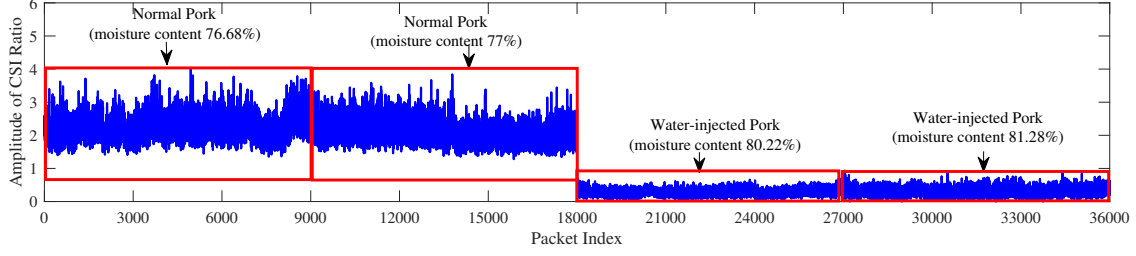


Fig. 8. Amplitude of the CSI ratio for four different pork samples.

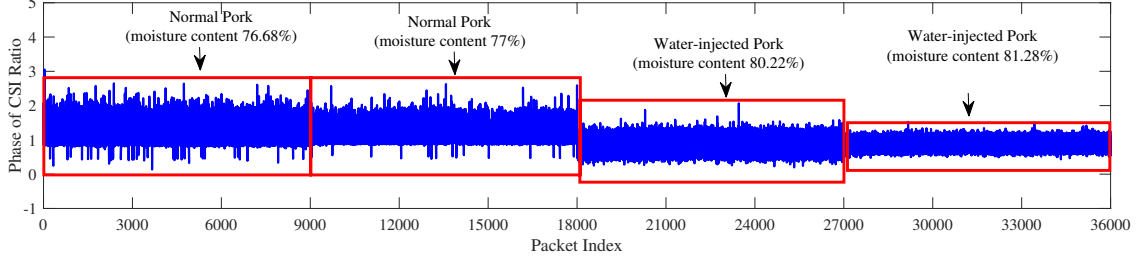


Fig. 9. Phase of CSI ratio for four different pork samples.

1) *Double-layer LSTM*: Compared with the recurrent neural network (RNN), LSTM can overcome the gradient vanish problem. LSTM also has a stronger nonlinear learning ability to extract features from complex high-dimensional data [20]. In our model, the LSTM network uses the preprocessed CSI ratio data for water-injected pork detection, in which the hidden LSTM unit can map the input CSI ratio data into output labels (i.e., normal pork or water-injected pork). As shown in Fig. 10, a double-layer LSTM network structure is used for water-injected pork detection for improved learning ability. We use the LSTM network to achieve the mapping from normalized CSI ratio data $\mathbf{v} = (v_1, v_2, \dots, v_T)$ to output label y at different time intervals from $t = 1$ to T , which is formulated by

$$i_t = \sigma(\omega_{ix}v_t + \omega_{im}h_{t-1} + b_i), \quad (8)$$

$$f_t = \sigma(\omega_{fx}v_t + \omega_{fm}h_{t-1} + b_f), \quad (9)$$

$$o_t = \sigma(\omega_{ox}v_t + \omega_{om}h_{t-1} + b_o), \quad (10)$$

$$g_t = \tanh(\omega_{cx}v_t + \omega_{cm}h_{t-1} + b_c), \quad (11)$$

$$c_t = f_t \odot c_{t-1} + i_t \odot g_t, \quad (12)$$

$$h_t = o_t \odot \tanh(c_t), \quad (13)$$

where ω is the weight matrix; the \mathbf{b} term is the bias vector; $\tanh(\cdot)$ is the hyperbolic tangent function, $\sigma(\cdot)$ is the sigmoid function; i , f , o , g , and c are the input gate, the forget gate, the output gate, the candidate value, and the unit activation, respectively; h represents the cell outputs for an activation vector; \odot is the element-wise product of vectors.

2) *Softmax Classifier*: In the double-layer LSTM network, its final output is fed into a fully connected layer, where we use a Softmax function to detect water-injected pork. Specifically, the output of the Softmax function is defined by $\mathbf{p} = [p_1, p_2, \dots, p_N]$, where N is the number of output neurons

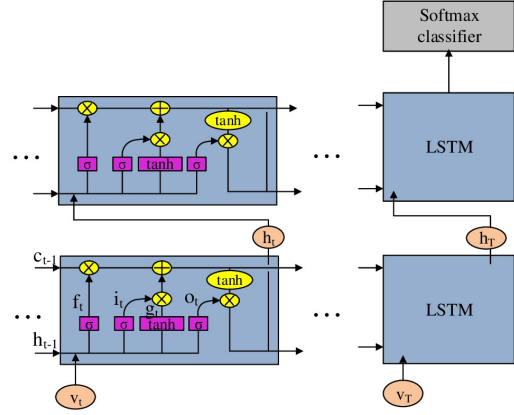


Fig. 10. Double-layer LSTM network structure.

in the Softmax function, which is defined as

$$p_i = \frac{e^{\mathbf{k}_f^T \omega_i}}{\sum_{n=1}^N e^{\mathbf{k}_f^T \omega_n}}, \quad i = 1, 2, \dots, N, \quad (14)$$

where ω_n is the weight vector of the fully connected layer, \mathbf{k}_f is the output vector of the final cell's hidden node in the second layer, and $(\cdot)^T$ is the transpose operator.

In the training stage, we define $F(\omega)$ as the loss function over weight ω . Meanwhile, we use cross entropy to measure the difference between output data and true labeled data. Regularization is utilized to reduce the solution space and

avoid over-fitting. The optimal ω is achieved by

$$\arg \max_{\omega} F(\omega) = - \sum_{i=1}^N y_i \log(p_i) + \frac{\eta}{2} \|\omega\|_2^2, \quad (15)$$

where y_i is the true label for the i th pork sample, and η is the hyperparameter for regularization. The back propagation through time (BPTT) algorithm is used for training the LSTM network, and the Adam optimizer is also used to improve the optimization efficiency.

D. Online Detection

In the online stage, we preprocess the M new CSI ratio data collected for the new pork sample, and then use the trained double-layer LSTM network model for online detection. For N different pork samples, the output O of the final Softmax classifier is given by

$$O = \begin{bmatrix} O_{11} & O_{12} & \cdots & O_{1M} \\ O_{21} & O_{22} & \cdots & O_{2M} \\ \vdots & \vdots & \ddots & \vdots \\ O_{N1} & O_{N2} & \cdots & O_{NM} \end{bmatrix}, \quad (16)$$

where O_{ij} represents the output probability for the i th pork sample sampled from the j th WiFi packet. To reduce the variance of the output, we calculate the average of the M output data of each pork sample, and use O_i to represent the average of the data vector $[O_{i1}, O_{i2}, \dots, O_{iM}]$ in the i th row. Therefore, the average vector is given by $\bar{O} = [\bar{O}_1, \bar{O}_2, \dots, \bar{O}_N]$. Finally, the water-injected pork test result R is predicted by

$$R = \underset{i \in \{1, 2, \dots, N\}}{\operatorname{argmax}} \bar{O}_i. \quad (17)$$

IV. IMPLEMENTATION, EXPERIMENTS AND DISCUSSIONS

In this section, the implementation of WiPd system is introduced in detail. We then evaluate the performance of WiPd through extensive experiments.

A. Sample Preparation

In our experiment, four pieces of fresh pork from the market were used. We first treated their connective tissues on the surface. Then according to the uniform size ($\approx 30\text{cm} \times 8\text{cm} \times 3\text{cm}$) and weight ($\approx 1\text{kg}$) standards, four pork samples were obtained. Two blocks were not injected with any water, while the other two blocks were injected with water according to 10% and 20% of their weight, respectively. Water was injected at 10 different locations in the port sample, while the spacing between two water injection points was about 3cm (so that the water injection points can be evenly distributed in the sample), and water was injected at a depth of about 1.5cm. After water injection, the sample was rested at room temperature for 30min to make the injected water evenly distributed inside the port. Finally, the sample was weighed. Fig. 11 shows the water injection action. Table I shows the changes of pork sample before and after water injection. The original moisture content and final moisture content in the Table I, i.e., the ground truth, were measured from the four pork samples using a high-temperature dryer (i.e., the SN-DHS-16 moisture dryer shown



Fig. 11. The water injection scenario.



Fig. 12. The SN-DHS-16 moisture dryer for ground truth.

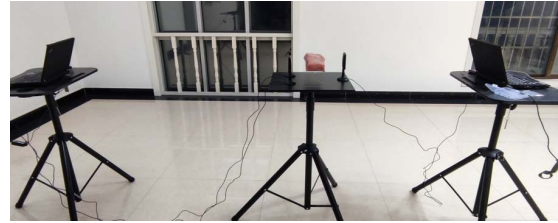


Fig. 13. The experimental scenario.

in Fig. 12), after collecting the CSI data and inference their states with WiPd.

B. WiPd Implementation

The hardware of our system consists of two Lenovo ThinkPad X201 notebook computers equipped with Intel 5300 NIC, where one computer using one antenna is the transmitter and the other using two antennas is the receiver. Both computers run the Ubuntu Linux 14.04 operating system, and MATLAB 2021b is used for data processing.

In order to test the effectiveness of our WiPd system, we conducted experiments in the LOS scenario. As shown in Fig. 13, different pork samples were placed in the middle of the LOS path to collect CSI data. In addition, we collected CSI data from 10,000 WiFi packets for each pork sample at a sampling rate of 1,000 packets/s, 40,000 CSI samples in total for the four port samples. Then, 7,000 CSI samples of each pork sample are randomly selected, and a total of 28,000 CSI samples are used to train the double-layer LSTM network model. The remaining CSI samples are used for testing.

C. Performance Evaluation

Fig. 14 shows the accuracy of water-injected pork detection in the LOS scenario using CSI ratio of amplitude data. We can see that the accuracy rates of all the four samples are

TABLE I
CHANGES OF PORK SAMPLE INDEXES BEFORE AND AFTER WATER INJECTION

Sample	Original moisture content ($\pm 0.5\%$)	Original weight	Injection rate	Weight after injection	Final moisture content ($\pm 0.5\%$)
1	76.68%	1.06kg	0%	1.06kg	76.68%
2	77%	1.04kg	0%	1.04kg	77%
3	77.46%	1kg	10%	1.08kg	80.22%
4	77.32%	1kg	20%	1.19kg	81.28%

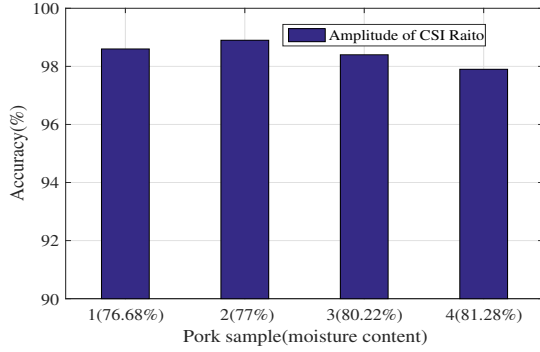


Fig. 14. Detection accuracy with CSI ratio of amplitude data.

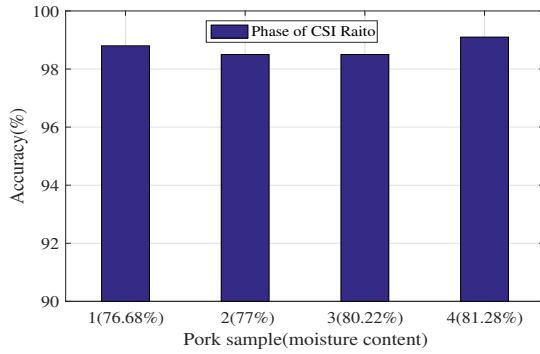


Fig. 15. Detection accuracy with CSI ratio of phase data.

more than 97%, and the accuracy rates of the two water-injected pork samples are 98.4% and 97.9%, respectively. Moreover, the average detection accuracy is about 98.4%. Fig. 15 shows the accuracy of water-injected pork detection in the LOS scenario using CSI ratio of phase data. Similarly, we find that the accuracy rate of the four samples are all more than 98%, and the accuracy rates of the two water-injected pork samples are 98.5% and 99.1%, respectively. The average detection accuracy is 98.7%. Therefore, the proposed WiPd system can be used for water-injection pork detection in the LoS scenario. Also, the CSI ratio of phase data has a better performance than the CSI ratio of amplitude data, because the calibrated phase is more robust in indoor environments.

D. Impact of System Parameters

To validate the impact of system parameters, we analyze and discuss different factors in the WiPd design, including different distances between transmitting and receiving antennas, different proportions of data packet training, different antenna

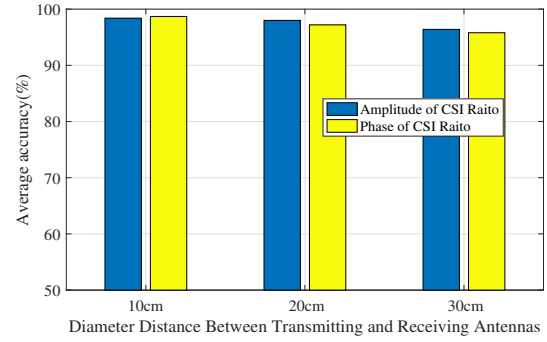


Fig. 16. Average detection accuracy for different transmitter-receiver distances.

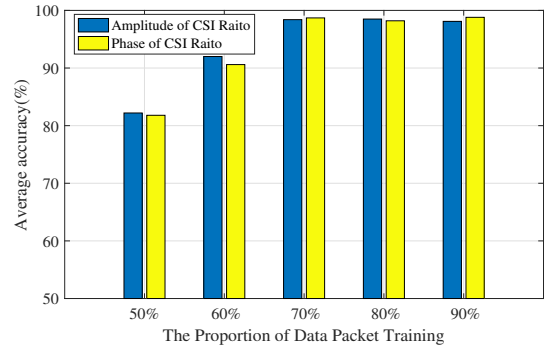


Fig. 17. Average detection accuracy in different portions of training and testing data.

types, different antenna pairs, different frequency bands, and different indoor environments. We also examine the system robustness in this section.

1) *Different Distances between Transmitting and Receiving Antennas:* Different distances between the transmitting and receiving antennas will have different multipath effects. Fig. 16 shows the average detection accuracy under different distances between transceiver antennas in the LoS scenario. It can be seen from the results in Fig. 16 that as the distance is increased, the average detection accuracy using the CSI ratio of amplitude data decreases from 98.4% to 96.4%. Using the CSI ratio of phase data, the average detection accuracy decreases from 98.7% to 95.8%. Although the increased distance will affect the performance of the system, but WiPd can always maintain a high accuracy of more than 90%.

2) *Different Amount of Training Data:* We use different proportions of training data and testing data to evaluate the

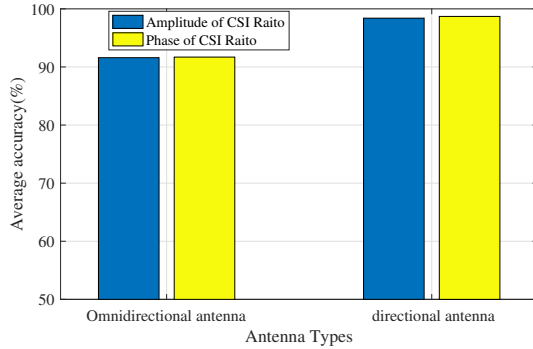


Fig. 18. Average detection accuracy using different types of antennas.

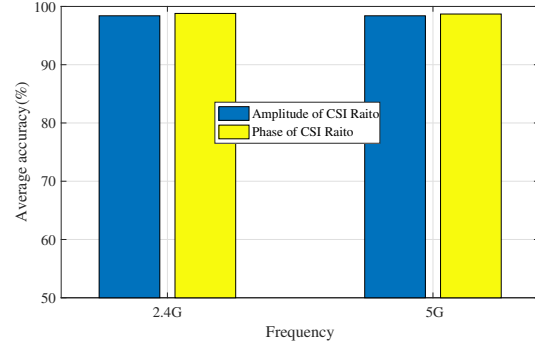


Fig. 20. Average detection accuracy in different frequency bands.

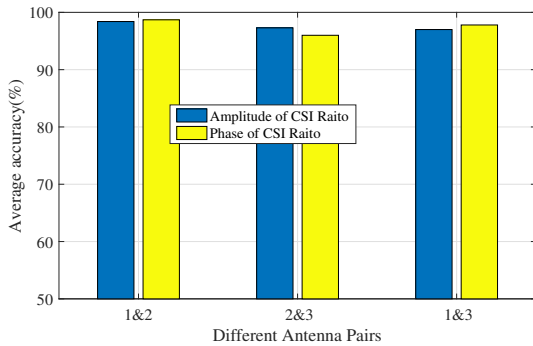


Fig. 19. Average detection accuracy using different paris of antennas.

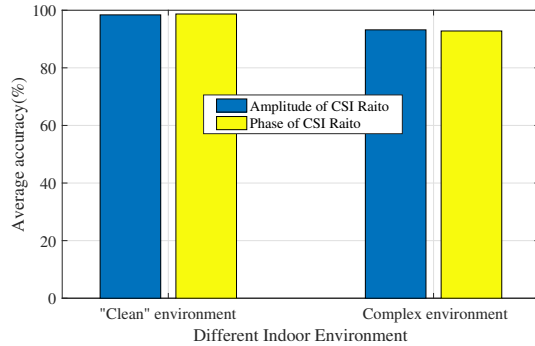


Fig. 21. Average detection accuracy in different indoor environments.

performance of the WiPd system. Fig. 17 shows the average detection accuracy for different proportions of training data and testing data in the LOS scenario. We can see that the average accuracy of the system is increased with the increase of the amount of training data, especially in the range from 50% to 70%. When we train with portions of more than 70%, 80%, and 90% of the CSI ratio of amplitude data, the system almost achieves the same average detection accuracy. Similarly, when we train with portions of more than 70%, 80%, and 90% of the CSI ratio phase data, the system also achieves similar average detection accuracy. Therefore, in the WiPd system, we use 70% of data for training the double-layer LSTM model.

3) *Different Antenna Types*: Different antenna types have an impact on the system performance. For example, omnidirectional antennas are usually more susceptible to the multipath effect and incur a larger environmental interference, while directional antennas focused towards the LOS path will have a smaller environmental interference. The results of using two different types antenna are presented in Fig. 18. It can be seen from Fig. 18 that the average detection accuracy rates of WiPd using the CSI ratio of amplitude data and the CSI ratio of phase data under directional antenna are both higher than that of the omnidirectional antenna, although the cost for two different types of antenna are almost the same. Therefore, we choose to use directional antenna in our WiPd system for

better performance.

4) *Different Antenna Pairs*: The Intel 5300 network card used in the WiPd system is equipped with three antenna interfaces. As shown in Fig. 19, we show the detection impact of different pairs of antennas. It can be seen that the combination of antenna 1 and antenna 2 is better than the other two combinations, because different antenna pairs experience different multipath noise and environmental noise, resulting in different stability. In the WiPd system, we choose a better antenna combination for water injected pork detection.

5) *Different Frequency Bands*: We next study the impact of different frequency bands on the WiPd system. Fig. 20 shows the detection accuracy of water injected pork in the two frequency bands, i.e., 2.4GHz and 5GHz, supported by the Intel 5300 NIC. It can be seen that the CSI data over different frequency bands are both effective. Under the two frequency bands, the average detection accuracy of WiPd is always more than 98%.

6) *Different Indoor Environments*: We evaluate the robustness of the system by collecting data in different indoor environments. Before our experiment, we collect data in a relatively "clean" environment, and next in a complex indoor environment. The complex environment has tables and other furniture in the surroundings to simulate our daily family kitchen environment. Fig. 21 shows the average test results for the two different environments. It can be seen that the performance of the system decreases in the complex home

TABLE II
PROPERTIES OF SEVEN FRESH PORK SAMPLES

Samples	1	2	3	4	5	6	7
Weight (kg)	1	1.5	2	1	1.5	1	2
Water Injection	no	no	no	no	yes	yes	yes

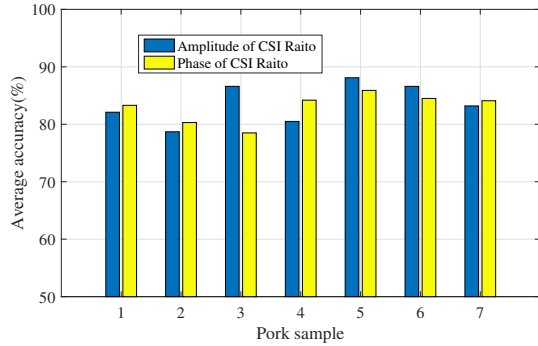


Fig. 22. Average detection accuracy for different fresh pork samples.

environment, because the impact of multipath is more serious in the complex environment. However, the detection accuracy of the system can still be maintained at about 90%, which is acceptable in practice.

7) *System Robustness*: Finally, we validate the robustness of the system. We use seven pieces of fresh pork without any treatment from the market, which are different in shape, size, and weight. Three of them are chosen for water injection. Then we directly collect the CSI data from the seven fresh pork samples. Finally, the trained model is used to detect water injected pork with the new CSI data. Table II shows the properties of the seven samples. As shown in Fig. 22, the detection results are acceptable. Even if we do not deal these properties of pork samples, the average detection accuracy of the system is almost more than 80%, which fully validates the robustness of the WiPd system.

V. CONCLUSIONS

In this paper, we introduced the WiPd system, a low-cost, non-contact water-injected pork detection system based on WiFi CSI. First, we validated the feasibility of water-injected pork detection through the CSI data collected using commercial WiFi devices. Then we developed the WiPd system design. The system included three parts: CSI data collection, data preprocessing, and detection model with a double-layer LSTM network. We carried out water-injected pork detection experiments, and the results verified the effectiveness of WiPd in different system parameters and test settings.

ACKNOWLEDGMENTS

This work is supported in part by the National Science Foundation of Henan (No.222300420004) and Major Public Welfare Special Projects of Henan Province (No.201300210100), National Natural Science Foundation of China (No. 62172141,61772173), the National Key Research

and Development Program of China (2017YFD0401001), Youth Innovative Talents Cultivation Fund Project of Kaifeng University in 2020 (KDQN-2020-GK002), and NSF (ECCS-1923163, CNS-2105416, and CNS-2107164).

REFERENCES

- [1] G. J. Peng, M. H. Chang, M. Fang, C. D. Liao, and H. F. Cheng, "Incidents of major food adulteration in Taiwan between 2011 and 2015," *Food Control*, vol. 72, no. Part A, pp. 145–152, Feb. 2017.
- [2] S. Nasreen and T. Ahmed, "Food adulteration and consumer awareness in Dhaka city, 1995-2011," *Journal of Health Population & Nutrition*, vol. 32, no. 3, pp. 452–464, Sept. 2014.
- [3] H. Wang *et al.*, "Effects of different drying methods on drying kinetics, physicochemical properties, microstructure, and energy consumption of potato (*solanum tuberosum l.*) cubes," *Drying Technology*, vol. 39, no. 3, pp. 418–431, Sept. 2020.
- [4] J. D. Pettinati, C. E. Swift, and E. H. Cohen, "Moisture and fat analysis of meat and meat products: A review and comparison of methods," *Journal - Association of Official Analytical Chemists*, vol. 56, no. 3, pp. 544–561, May 1973.
- [5] Fabola, Manhas, Verbi, Pereira, Luiz, Alberto, and Colnago, "Determination of the moisture content in beef without weighing using benchtop time-domain nuclear magnetic resonance spectrometer and chemometrics," *Food Analytical Methods*, vol. 3, pp. 1349–1353, Mar. 2012.
- [6] J. X. Wang, L. F. Fan, H. H. Wang, P. F. Zhao, H. Li, Z. Y. Wang, and L. Huang, "Determination of the moisture content of fresh meat using visible and near-infrared spatially resolved reflectance spectroscopy," *Biosystems Engineering*, vol. 162, pp. 40–56, Oct. 2017.
- [7] J. Ma, D. W. Sun, and H. Pu, "Spectral absorption index in hyperspectral image analysis for predicting moisture contents in pork longissimus dorsi muscles," *Food chemistry*, vol. 197, no. Pt.A, pp. 848–854, Apr. 2016.
- [8] J. Gang, X. Liu, H. Guo, W. Ying, and Y. Liang, "Study of water-injected pork and pork freshness using microwave techniques," in *Proc. 9th Int. Symp. Antennas, Propagation and EM Theory*, Guangzhou, China, Nov.-Dec. 2011, pp. 614–617.
- [9] P. Bahl and V. N. Padmanabhan, "RADAR: An in-building rf-based user location and tracking system," in *Proc. IEEE INFOCOM 2000*, Tel Aviv, Israel, Mar. 2000, pp. 775–784.
- [10] X. Wang, C. Yang, and S. Mao, "On CSI-based vital sign monitoring using commodity wifi," *ACM Transactions on Computing for Healthcare*, vol. 1, no. 3, pp. 12:1–12:27, Apr. 2020.
- [11] X. Wang, X. Wang, and S. Mao, "Indoor fingerprinting with bimodal CSI tensors: A deep residual sharing learning approach," *IEEE Internet of Things Journal*, vol. 8, no. 6, pp. 4498–4513, Mar. 2021.
- [12] J. Ding and R. Chandra, "Towards low cost soil sensing using Wi-Fi," in *Proc. ACM Mobicom 2019*, Los Cabos, Mexico, Oct. 2019, pp. 1–16.
- [13] C. Li, M. Liu, and Z. Cao, "WiHF: Enable user identified gesture recognition with WiFi," in *Proc. IEEE INFOCOM 2020*, Tel Aviv, Israel, Mar. 2020, pp. 586–595.
- [14] W. Yang, X. Wang, A. Song, and S. Mao, "Wi-Wheat: Contact-free wheat moisture detection using commodity WiFi," in *Proc. IEEE ICC 2018*, Kansas City, MO, May 2018, pp. 1–6.
- [15] P. Hu, W. Yang, X. Wang, and S. Mao, "MiFi: Device-free wheat mildew detection using off-the-shelf WiFi devices," in *Proc. IEEE GLOBECOM 2019*, Waikoloa, HI, Dec. 2019, pp. 1–6.
- [16] W. Yang, E. Shen, X. Wang, S. Mao, Y. Gong, and P. Hu, "Wi-Wheat+: Contact-free wheat moisture sensing with commodity WiFi based on entropy," *Elsevier/KeAi Digital Communications and Networks*, 2022, to appear. DOI: 10.1016/j.dcan.2022.03.014.
- [17] Z. Jiang *et al.*, "Eliminating the barriers: Demystifying Wi-Fi baseband design and introducing the PicoScenes Wi-Fi sensing platform," *IEEE Internet of Things J.*, vol. 9, no. 6, pp. 4476–4496, Mar. 2021.
- [18] D. Wu, Y. Zeng, F. Zhang, and D. Zhang, "WiFi CSI-based device-free sensing: from Fresnel zone model to CSI-ratio model," *CCF Trans. Pervasive Computing and Interaction*, pp. 88–102, 2022.
- [19] C. Feng, J. Xiong, L. Chang, J. Wang, X. Chen, D. Fang, and Z. Tang, "WiMi: Target material identification with commodity Wi-Fi devices," in *Proc. IEEE ICDCS 2019*, Dallas, TX, July 2019, pp. 700–710.
- [20] W. Yang, X. Wang, S. Cao, H. Wang, and S. Mao, "Multi-class wheat moisture detection with 5GHz Wi-Fi: A deep LSTM approach," in *Proc. ICCCN 2018*, Hangzhou, China, July/Aug. 2018, pp. 1–9.